Fifth International Symposium on Marine Propulsors
smp'17, Espoo, Finland, June 2017

The numerical prediction of the propeller cavitation and hull pressure fluctuation in the ship stern using OpenFOAM

Zheng Chaosheng[1]

[1] China Ship Scientific Research Center (CSSRC) national key laboratory on ship vibration & noise, Jiangsu Key laboratory of Green Ship technology, Wuxi, Jiangsu, China

ABSTRACT

The numerical prediction method of the propeller cavitation and hull pressure fluctuation in the ship stern is set up in the paper using unsteady viscous RANS approach and SchnerrSauer cavitation model using OpenFOAM, which is an open-source CFD platform. Then the propeller cavitation and hull pressure fluctuation induced at both design draft condition and ballast draft condition are predicted respectively. The cavitation shape and the amplitudes of the first blade frequency (1BF) of the hull pressure fluctuation show good agreement with the experiment observations and measurements. The modification of the turbulence viscosity for cavitating flows is applied to investigate the effects on the hull pressure fluctuation as well.

Keywords

OpenFOAM, propeller cavitation, pressure fluctuation

1 INTRODUCTION

The viscous RANS approach has been used for the flow simulation around propeller widely since 1980s, the early work of cavitation simulation targets hydrofoil and underwater vehicle, and has been accomplished mainly by commercial CFD solvers. As one important aspect of propeller performance, the propeller cavitation has been studied by numerical simulation method, and some research papers come in public. Da-Qing Li (2012) has predicted the E779A cavitation in non-uniform wake based on RANS approach and Zwart cavitation model using ANSYS FLUENT. Kwang-Jun Paik (2013) has predicted the propeller cavitation pattern and the hull pressure fluctuation induced, using FLUENT and SchnerrSauer cavitation model.

Recently, the open-source CFD platform, OpenFOAM has been increasingly popular in the numerical simulation of propeller cavitation. Abolfazl (2015) has predicted the PPTC propeller cavity extent within a 12°inclination of shaft using ILES method and SchnerrSauer cavitation model based on OpenFOAM. Rickard E Bensow (2015) has studied the cavity extent, flow field and forces on the propeller of a 7000 DWT chemical tanker, with ILES method and Kunz cavitation model adopted in OpenFOAM. Zheng Chaosheng (2016) has predicted the unsteady propeller cavitation behind a 82,000 DWT bulk carrier using RANS method and OpenFOAM, and the cavitation shape change shows good agreement with the experiment observations.

The present work aims to predict the unsteady propeller cavitation in the stern region of a single-screw container vessel, with special attention to the unsteady cavitation behavior and the influence of the turbulence viscosity modification on the hull pressure fluctuation.

2 NUMERICAL METHODS AND MODELS

2.1 Governing equations

The unsteady RANS approach is adopted because of the significantly lower computational effort than LES.

$$\frac{\partial \rho}{\partial t} + \nabla(\rho U) = 0 \tag{1}$$

$$\frac{\partial \rho U}{\partial t} + U \cdot \nabla(\rho U) = \nabla \cdot \left((\mu + \mu_t)\nabla U\right) - \nabla p - F_s \tag{2}$$

The turbulent viscosity μ_t is modeled by the SST $\kappa\omega$ turbulence model together with wall functions.

In the VOF approach, the physical properties of the fluid are scaled by the liquid volume fraction γ, with $\gamma = 1$ corresponding to pure water.

The density and dynamic viscosity of the fluid are scaled as

$$\rho = \gamma\rho_l + (1-\gamma)\rho_v \tag{3}$$

$$\mu = \gamma\mu_l + (1-\gamma)\mu_v \tag{4}$$

The mass transfer equation of the liquid volume fraction γ can be written as

$$\frac{D\gamma}{Dt} = \frac{\partial \gamma}{\partial t} + \nabla \cdot (\gamma U) = \frac{\dot{m}}{\rho_l} \tag{5}$$

where the mass transfer rate $\dot{m}$ is to be modeled by cavitation models.

The transport Equation (1) for mass (continuity equation) can be re-written in combination with Equation (1), Equation (3) and Equation (5).

$$\nabla \cdot U = \dot{m}(\frac{1}{\rho_l} - \frac{1}{\rho_v}) \quad (6)$$

It implies that the cavitation model is involved in the coupling procedure of velocity and pressure. For the cavitation flow simulations, the sources of the mass transfer equation are computed in the PISO loop firstly, then the volume fraction transport of the vapour is progressed, and the standard PISO procedure is entered.

2.2 Cavitation model

Cavitation is the transition of liquid into vapour in the low pressure regions caused by the presence of small gas nuclei in the fluid. The SchnerrSauer cavitation mass transfer model is employed to mimic the phase change between vapour and liquid, and already implemented in OpenFOAM.

$$\dot{m} = sign(p_v - p)\frac{n_0}{1 + n_0 \frac{4}{3}\pi R^3} 4\pi R^2 \sqrt{\frac{2}{3}\frac{|p_v - p|}{\rho_l}} \quad (7)$$

where n_0 stands for the number density of micro bubbles per liquid volume and R is the initial nuclei radius. SchnerrSauer's model is based on bubble dynamics by considering the equation of motion of a single bubble of radius R.

2.3 Discretization and solution procedure

The finite volume method is used for the discretization of the governing equations, and the unsolved flow variables are stored in the cell-centre positions in the computational grid. The Euler differencing scheme is used for the time discretization, and a second order differencing scheme is adopted for the components of the momentum equation.

The interPhaseChangeDyMFoam solver used in this study is a multiphase solver, taking two fluids into account using the VOF method.

To improve the convergency of the cavitation flow and reduce the computational time, the full wetted flow is simulated using MRF method at first, after obtaining a quasi-stable flow field, the sliding mesh is then applied to simulate the rotation of propeller. The three components of the momentum equation are solved sequentially in a loop within each time step. The PIMPLE algorithm is applied for the coupling between the velocity and the pressure fields, allowing for stable transient simulations with $\max Co \geq 1$. The PIMPLE algorithm is a combination of the SIMPLE and PISO algorithms, where the PISO loop is complemented by an outer iteration loop and the under-relaxation of the variables.

3 BOUNDARY CONDITIONS AND MESH GENERATION

The configuration investigated here is an 14000 TEU container vessel, which is a single screw vessel, driven by a fixed pitch six-bladed propeller. The experiment of cavitation observation and measurement for the model propeller is performed in the large cavitation channel of China Ship Scientific Research Center. The principle parameters of model propeller is provided in Table 1, and the hull and propeller are visualised in Figure 1.

Table 1 The principle parameters of model propeller

Propeller diameter, D	0.25263m
Pitch-diameter ratio, P/D	1.0729
Skew angle	36.8°
Expanded area ratio, EAR	0.8
Number of blades, Z	6
Scale ratio, λ	38

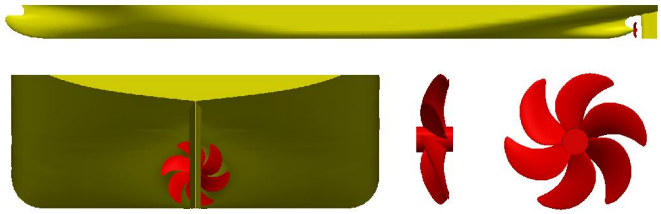

Figure 1 The 14000 TEU container vessel and propeller

The experiment setup inside the cavitation tunnel is shown in Figure 2. The initial rotation angle φ is defined as 0° at 12 o' clock.

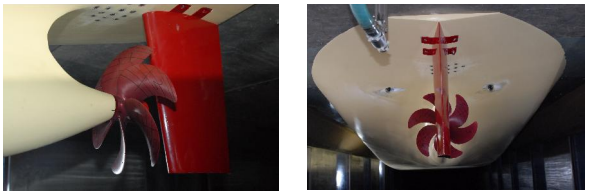

Figure 2 The experiment setup

The inlet boundary is defined as velocity inlet condition with a fixed value of velocity U. The outlet boundary defined as pressure outlet condition, and the pressure value is constant based on the cavitation number σ_n. The hull, propeller, rudder and hub boundary are defined as no-slip wall conditions, respectively.

The mesh is generated using HEXPRESS. The computational domain is divided into two sub-regions. The ship region contains the flow region that includes the inlet, outlet, ship and rudder, the propeller region is a small cylinder surrounding the propeller. The grid of the two sub-regions all consist of unstructured hexahedral cells, and a number of the boundary layer cells are inserted, the non-dimensional parameter of the hull, Y+ ≈110. The ship region and propeller region are consist of 5.51 million and 1.01 million cells, respectively. The overview of surface mesh is shown in Figure 3. The interpolation between the non-conforming interfaces of the two sub-regions is implemented in OpenFOAM, named as AMI (Arbitrary Mesh Interface).

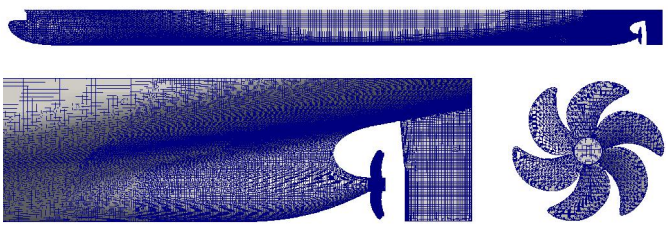

Figure 3 The overview of surface mesh

4 RESULTS AND DISCUSSIONS

The test conditions of the cavitation observation and measurement in this study is summarized in Table 2.

Table 2 The test conditions

	Design draft	Ballast draft
n	28rps	28rps
$\sigma_{n0.8R}$	0.3397	0.2493
KT	0.1989	0.1887

where n is the rotational speed of the propeller, $\sigma_{n0.8R}$ is the cavitation number, and K_T is the thrust coefficient. The definitions are as follows:

$$\sigma_{n0.8R} = \frac{p - p_v}{0.5\rho(0.8\pi nD)^2} \tag{8}$$

$$K_T = \frac{T}{\rho n^2 D^4} \tag{9}$$

Note that the grid of computational region is prepared according to design draft, and not changed for ballast draft condition. Instead of this, the ballast condition is considered by KT-identity method and adjustment of the channel pressure to the corresponding cavitation number.

Firstly, the steady full wetted flow is simulated using MRF method to obtain a quasi-stable flow field, then the unsteady computation is started to simulate the rotation of propeller using sliding mesh method, and the cavitation model is activated to predict the cavitation, finally. The parameters in SchnerrSauer cavitation model are selected as $n_0=2\times10^8$, $d_{Nuc}=1\times10^{-4}$.

The predicted cavitation in the stern region at design and ballast draft is compared with the experiment sketches side-by-side in Figure 4 and Figure 5, respectively.

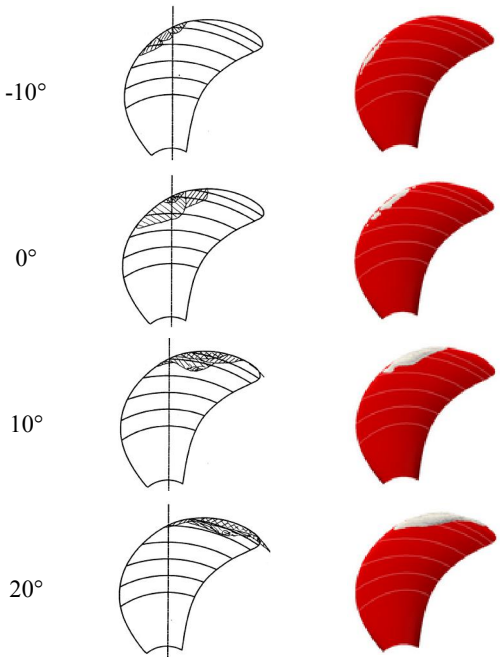

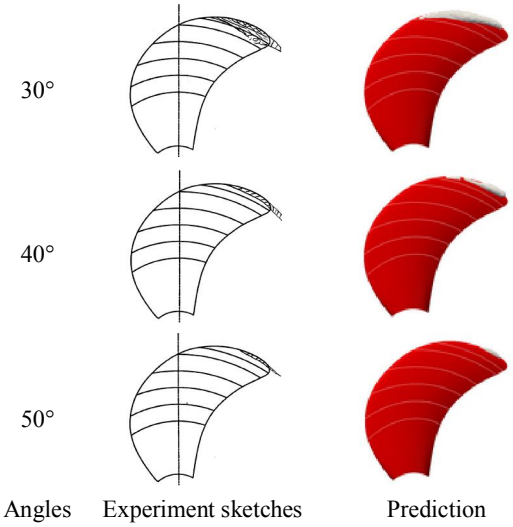

Figure 4 The experiment sketches vs. prediction at design draft condition

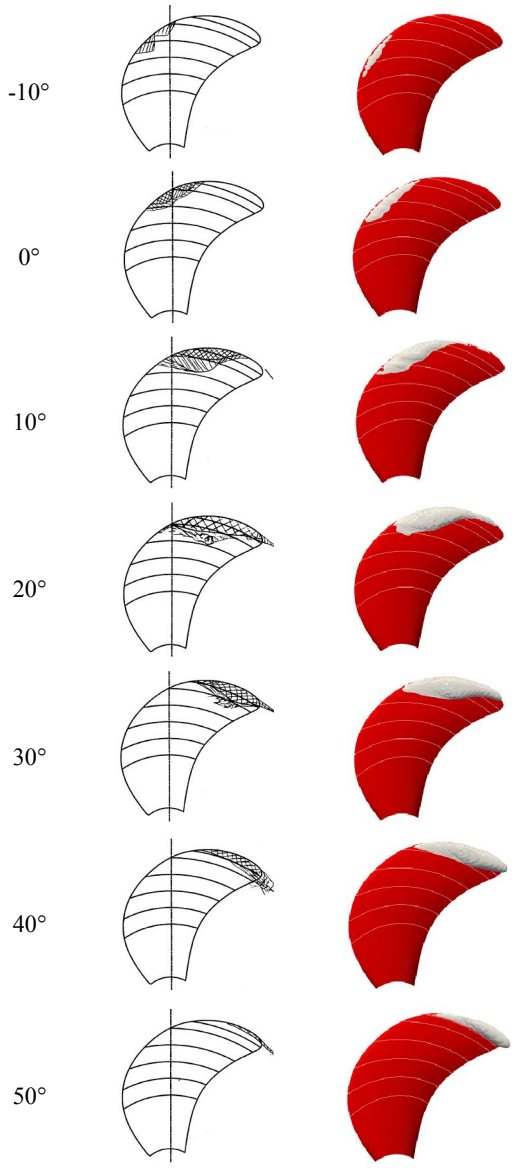

Figure 5 The experiment sketches vs. prediction at ballast draft condition

In Figure 4 and Figure 5, the predicted cavity, represented by vapour iso-surface of 0.1 shows the same behaviour as the experiment observations. The key feature, the extent change of the attached cavity with the rotation angles and the collapse at the tail of the main cavity, correlates well with the experiment, e.g. the cavity begins at about the same location φ≈-10°, reaches the maximum area at φ≈10° at design draft condition, and at φ≈20° at ballast draft condition. Nevertheless, since the mesh resolution around the blade tip is not enough, the tip vortex cavity cannot be predicted.

In order to investigate the hull pressure fluctuation induced by cavitation, the monitor points are arranged on the stern surface shown in Figure 6.

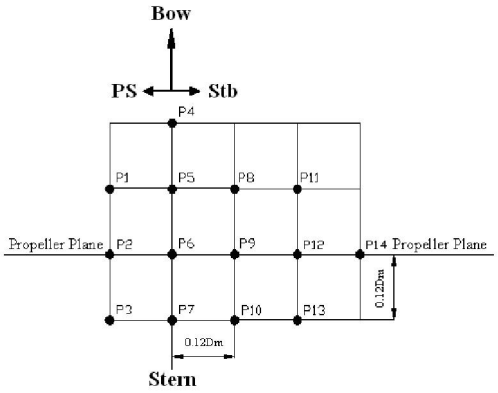

Figure 6 The arrangement of monitor points

The pressure fluctuation predicted at model scale is analysed by FFT, and converted to the pressure fluctuation at full scale by the formula. The amplitudes of the first blade frequency (1BF) of the hull pressure fluctuation predicted at ballast draft condition is compared with the experiment in Figure 7. The prediction shows good agreement with the test measurement, and the spatial laws of the pressure fluctuation is predicted well, and the maximum value of the 1BF pressure fluctuation is at P9.

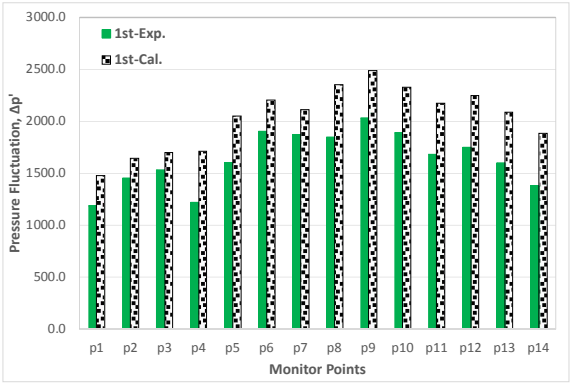

Figure 7 The 1BF of hull pressure fluctuation predicted vs. the experiment at ballast draft condition

Furthermore, the second and third blade frequency are compared with the experiment in Figure 8 and Figure 9, respectively. The obvious differences indicate that the instability of the propeller cavitation at the same angle in different period is not well captured, and needed to be further studied in the future.

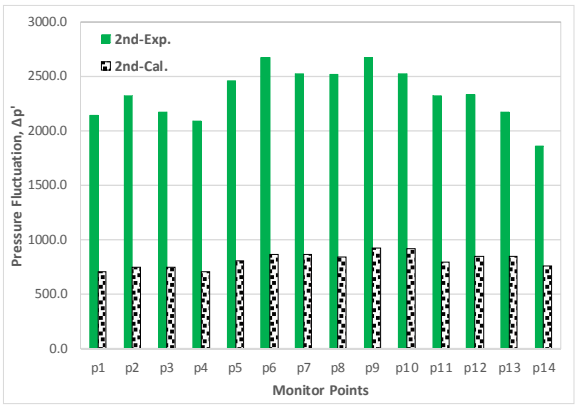

Figure 8 The 2BF of hull pressure fluctuation predicted vs. the experiment at ballast draft condition

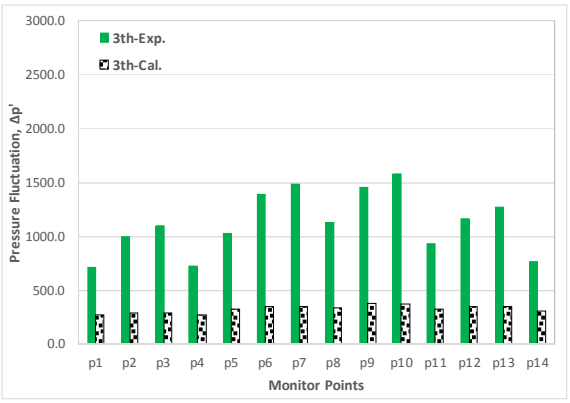

Figure 9 The 3BF of hull pressure fluctuation predicted vs. the experiment at ballast draft condition

Considering the great difference in density between water and vapour, the turbulence viscosity is modified according to the expression below:

$$\mu_t = f(\rho)\frac{a_1\kappa}{\max(a_1\omega, SF_2)} \tag{10}$$

$$f(\rho) = \rho_v + \frac{(\rho-\rho_v)^n}{(\rho_l-\rho_v)^{n-1}} \quad (n>1) \tag{11}$$

where the constant n is defined as 10.

After the modification, the turbulence viscosity on the blade at r=0.9R, φ=20° at ballast draft condition is compared with the before one in Figure 10, where $\nu_t = \mu_t/\rho$.

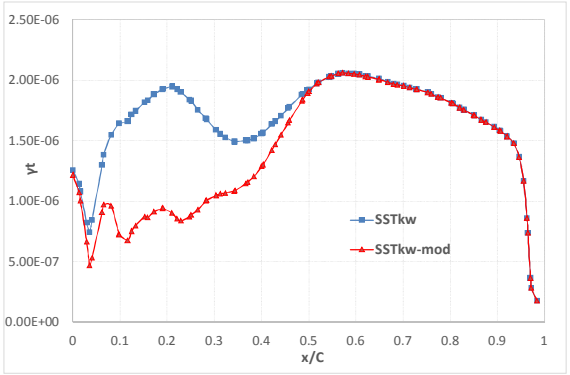

Figure 10 The turbulence viscosity before and after modification at r=0.9R, φ=20° at ballast draft condition

In Figure 10, it illustrates that the viscosity is reduced obviously in the region where vapour is dominant (between x/C=0～0.4).

The hull pressure fluctuation after the viscosity modification at ballast draft condition is compared with the before one in Figure 11. It seems that the modification of the turbulence viscosity has little effect on the value of the 1BF of the hull pressure fluctuation.

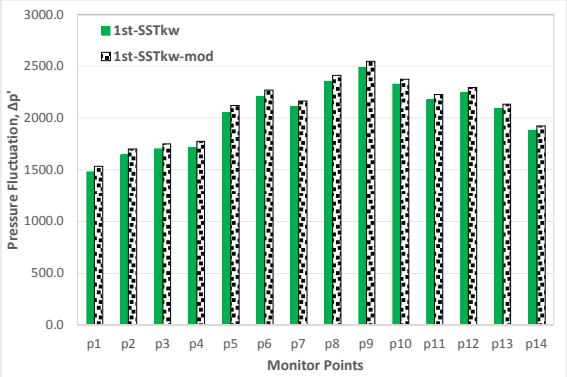

Figure 11 The 1BF of hull pressure fluctuation predicted before and after modification at ballast draft condition

5 CONCLUSIONS

In the stern region, The propeller cavitation shape and the amplitudes of the first blade frequency (1BF) of the hull pressure fluctuation predicted resemble well with the experiment observations and measurements. The prediction also finds that the modification of the turbulence viscosity which considering the great difference in density between water and vapour, has little effect on the value of the 1BF of the hull pressure fluctuation.

ACKNOWLEDGMENTS

This work is financially supported by National Natural Science Foundation of China (Project NO. 11332009).

REFERENCES

TANG D H, CHEN J D, ZHOU W X. (1998) . 'Comparative calculationsof propeller performance by RANS /Panel Menthod'. 22nd ITTC Propulsion Committee Propeller RANS/Panel Method Workshop, Grenble

CHEN J D, ZHOU W X, TANG D H, et al. (1998) . 'Comparative calculations of unsteady propeller performance by panel menthod'. 22nd ITTC Propulsion Committee Propeller RANS/Panel Method Workshop, Grenble

Da-Qing Li. (2012) . 'Prediction of Cavitation for the INSEAN Propeller E779A Operating in Uniform Flow and Non-Uniform Wakes'. 8th International Symposium on Cavitation, Singapore, pp.368-373

Kwang-Jun Paik. (2013) . 'URANS Simulations of Cavitation and Hull Pressure Fluctuation for Marine Propeller with Hull Interaction'. 3nd International Symposium on Marine Propulsors, Tasmania, pp.389-396

Abolfazl Asnaghi. (2015) . 'Computational Analysis of Cavitating Marine Propeller Performance using OpenFOAM'. 4th International Symposium on Marine Propulsors, Tesas, pp.148-155

Rickard E Bensow. (2015) . 'Large Eddy Simulation of a Cavitating Propeller Operating in Behind Conditions with and without Pre-Swirl Stators'. 4th International Symposium on Marine Propulsors, Tesas, pp.458-477

Zheng Chaosheng. (2016) . 'The unsteady numerical simulation of propeller cavitation behind a single-screw transport ship using OpenFOAM'. 2nd Conference of Global Chinese Scholars on Hydrodynamics, Wuxi, pp.117-123